NEAR-IR BROADBAND POLARIZER DESIGN BASED ON PHOTONIC CRYSTALS

Bogdan Stefaniță CALIN[1], Liliana PREDA[2]

We have successfully designed a broadband linear polarizer using a single photonic crystal, which acts in the wavelength interval of 0.66 – 1.9 μm. In this article we present a photonic crystal structure in which we studied the evolution of photonic band structures and transmissions for different modes of propagation, transverse electric (TE) and transverse magnetic (TM), with respect to the refractive indices, material thicknesses and peak heights. We have also developed a flexible method of designing similar structures employing these three parameters.

Keywords: photonic crystal, broadband linear polarizer, near-infrared, polarization filter

1. Introduction

A possible use for a broadband IR linear polarizer represents a filter for a polarization imaging sensor. Most imaging sensors today use only two of the three fundamental properties of light, which are color and intensity. Lately, more and more polarization imaging sensors are under development for both research and industrial applications. Among most recent studies on this subject we can mention studies made by Viktor Gruev in which they used polarizing optical filters made from aluminum nanowires [1], [2]. As far as photonic crystals are concerned, most studies are emphasized on methods of production [3], [4], with a tendency on applications that involve optical waveguides [5], beam splitters [6], polarization selective grating [6], optical resonators [7] and others.

The purpose of this paper is the study of a photonic crystal that can act as a broadband linear polarizer, and on finding an optimal geometry for such a structure. Using an appropriate substrate configuration we can produce a matrix of photonic crystal linear polarizers for different directions. In other words, we can produce the whole filter, which has different polarization directions for different pixels of a charge coupled device (CCD) using a single crystal. An example of an arrangement for these polarizers, based on Bayer filter [8], can be found in [9].

[1] PhD Student, Physics Department, University POLITEHNICA of Bucharest, Romania, e-mail: bogdan.calin@physics.pub.ro
[2] Lecturer, Physics Department, University POLITEHNICA of Bucharest, Romania

2. Design of a photonic crystal

For the design and simulations we used the OptiFDTD software package (version 11.2), a CAD environment that enables the design and simulation of advanced passive and non-linear photonic components, coupled with a LabVIEW application which was developed with the purpose of calculating the necessary geometrical parameters.

The photonic crystal is made of alternating films of different thickness and material. As we want to obtain a broadband linear polarizer, we need a high number photonic band gaps, distributed appropriately, therefore the photonic atom has two peaks of different heights in order to introduce a lower level of symmetry as it can be observed in figure 2 f). A photonic atom is defined in analogy with the atoms and/or molecules of the primitive cell in a regular (solid state) crystal, and it is comprised of at least two macroscopic media with differing dielectric constants.In the OptiFDTD version we used (11.2), we did not have many geometrical resources when designing the photonic atom and, therefore, we had to resort to alternatives, keeping the number of input parameters to a minimum in order to develop a flexible and easy-to-use design method. In order to construct one peak of the photonic atom, we used a series of 4 identical isosceles trapezoids as represented in figure 2. The symmetry properties of isosceles trapezoids not only allows the use of a minimum number of input parameters, but also offers the possibility of designing peaks of any dimensions using exactly the same application. All the geometrical parameters were calculated using basic linear equations and cartesian coordinates relative to the primitive cell. In short, an isosceles trapezoid in OptiFDTD is defined by the lengths of its bases and the cartesian coordinates of center of those bases. We know the dimensions of the photonic atom and the relative position of each trapezoid, and we use these relations to calculate the geometrical parameters specific for OptiFDTD. Once we have the dimensions for one trapezoid, we can construct the whole “ribbon” that represents a material film of the photonic atom by using 3 more copies of this trapezoid, positioned accordingly. Furthermore, we can split the photonic atom into several rectangles if we want it to have multiple peaks. The design steps of a photonic atom, after calculating the geometrical parameters of a trapezoid, are represented in figure 2, a) to e).

In other words, once we calculated the parameters required by OptiFDTD for the first trapezoid, we can quickly determine the other 3 and therefore define one peak.

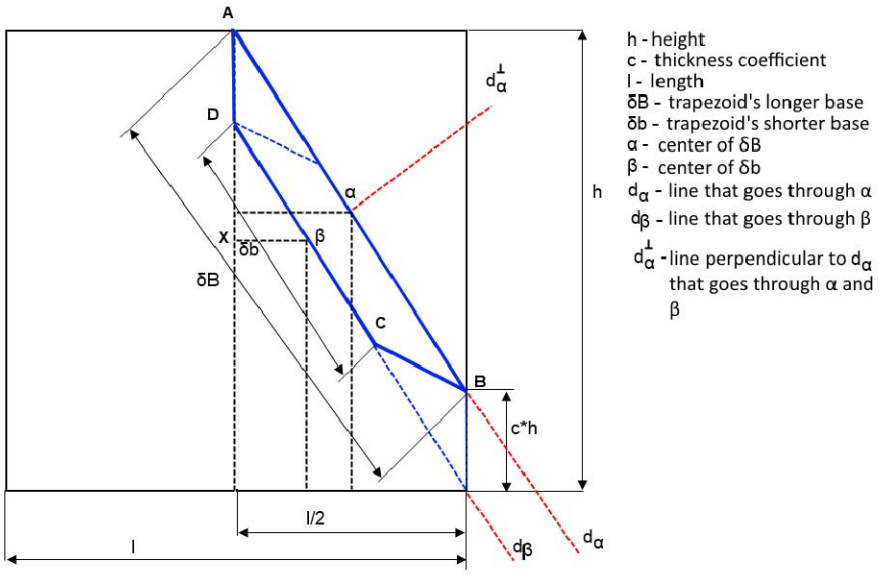

Fig. 1: Definition of the first isosceles trapezoid in the peak-fixing rectangle of the photonic atom.

In order to define a peak, we go through the following steps, presented as a summary of the whole rationale:

- We determine the line equation for d_α which contains the α point;
- We determine the vertical coordinate for α;
- We determine the equation for the line perpendicular to d_α, that goes through α, denoted as $d_\alpha^\perp$;
- We determine the line equation for d_β, which contains β;
- We determine the coordinates for β from the intersection $d_\alpha^\perp \cap d_\beta$;
- We determine the bases dimensions, therefore determining the first trapezoid (fig. 2a));
- We determine the geometrical parameters for the second trapezoid, which are now easier to calculate due to the symmetry of the structure (fig. 2b));
- We finally determine the geometrical parameters for the last two trapezoids, which represent the mirrored version of the first two trapezoids, with respect to one of the peak-fixing rectangle's symmetry axis (fig. 2c), 2d));
- We add the determined peak (fig. 2e)) to the photonic atom (fig. 2f));

To achieve this, we developed a simple LabVIEW application. There are 3 input parameters: the height and length of the rectangle that localizes the peak, and a thickness coefficient which represents a percentage of the rectangle's height. After the input data is typed in, simply running the application displays the

necessary geometrical parameters. The results from this application can be further implemented into a script to fully automate the design process specifically for OptiFDTD. This application helped with finding the optimal geometry of the crystal and it can be used for the design of any other similar structure. Examples of other similar structures designed using this application can be observed in figure 3.

The parameters we varied are the refractive indices, the material thickness and the height of one of the peaks. The higher refractive index, n_2, was varied between 3.3 and 3.7, while the lower refractive index, n_1, remained constant, with a value of n_1=1.4481. The thickness of one of the materials was varied between 0.09 µm and 0.45 µm, while the other material had a complementary variable thickness, as the sum of both thicknesses was constant and equal to 0.6 µm. The height of one of the peaks was varied between 0.35 µm and 0.55 µm, while the other peak had a constant height of 0.9 µm.

For the optimal geometry, the refractive indices were chosen for values of n_1=1.4481 and n_2=3.5 as the crystal yields better results with a higher refractive index contrast. In order to construct one peak, it must first be localized in a rectangle, as it can be observed in figure 2.

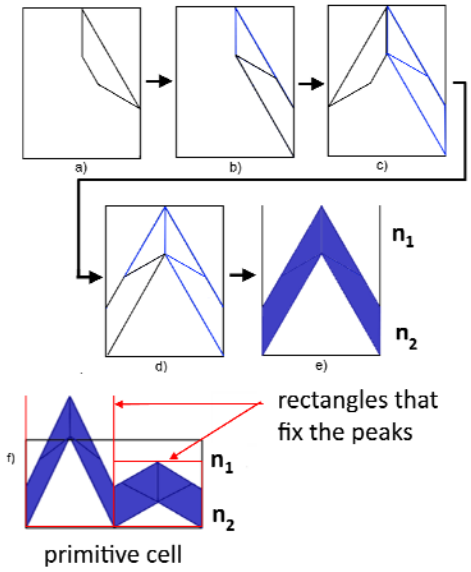

Fig. 2: Primitive cell design steps and materials, as they are computed in the LabVIEW application

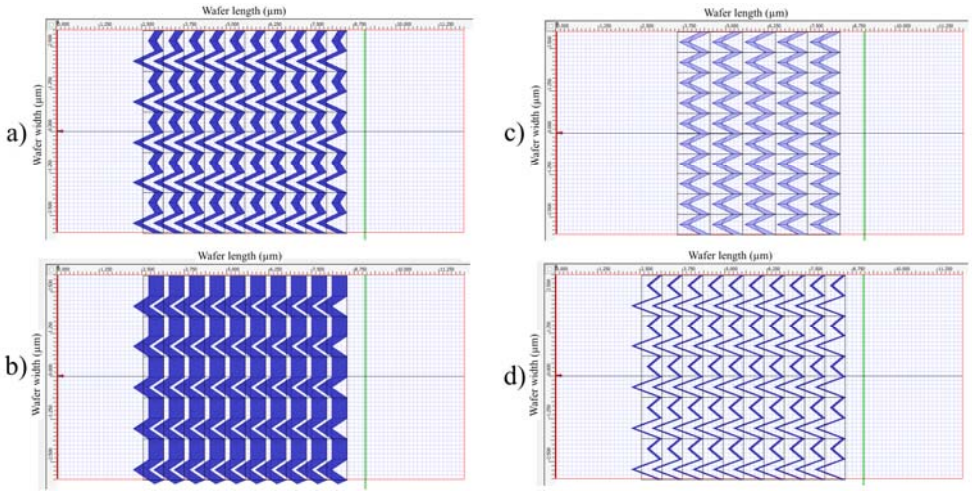

Fig. 3: Examples of similar structures whose geometrical parameters were calculated using the developed LabVIEW application: a) the optimal geometry for this study, b) single peak photonic atom, c) peak with straight band attached to the side, d) very thin peaks

It is possible for this rectangle to coincide with the photonic atom, but it is not necessary. The final (optimal) structure can be observed in figure 3 a). The light source is a plane Gaussian modulated continuous wave source with a homogenous intensity distribution over the width of the wafer.

For the light to be polarized upon traversing the crystal, it needs to present a low transmission for one of the propagation modes, transverse electric (TE) or transverse magnetic (TM), and a high transmission for the other. We calculated the band structure of a given crystal, for each propagation mode, using the Plane Wave Expansion method (PWE) in OptiFDTD. The photonic band structures were used to determine the approximate geometry, and the results were verified and fine-tuned based on the transmission spectra.

3. Results and discussions

One of the advantages of photonic crystals consists in the lack of constrains with respect to dimensions, so that a crystal can be scaled in order to modify the frequency band in which it acts. A linear relation can be established between a crystal's photonic band gaps and its scale, of the following form:

$$2 \cdot \frac{\omega}{2\pi c} = \frac{1}{2}\Gamma \tag{1}$$

where ω is the frequency, c is the speed of light and Γ is a scaling coefficient. Considering this fact, once we obtained a crystal with low transmission for TE and relatively high transmission for TM over a large interval, we modified its scaling in order to localize the effect over the desired wavelength interval.

We have plotted the data regarding the photonic band gap widths with respect to the three parameters (refractive index, thickness and second peak's height), which can be observed in figures 4 to 6. Based on this information, we started searching for an optimal geometry around the middle point, which is a structure with the highest refractive index contrast considering materials which make its production viable (Si with n_{Si}=3.5 and SiO_2 with n_{SiO2}=1.4281), a thickness of 0.27 μm and peak heights of 0.9 μm and 0.45 μm respectively. All band gaps are denoted in correlation with the transmission frequency bands between which they appear. For example, "b2-3" represents the frequency interval, known as "band gap", that appears between the second and the third transmission bands. The whole study was conducted for wavelengths in the interval 0.66 – 2 μm, and any band gap falling outside this interval was not considered.

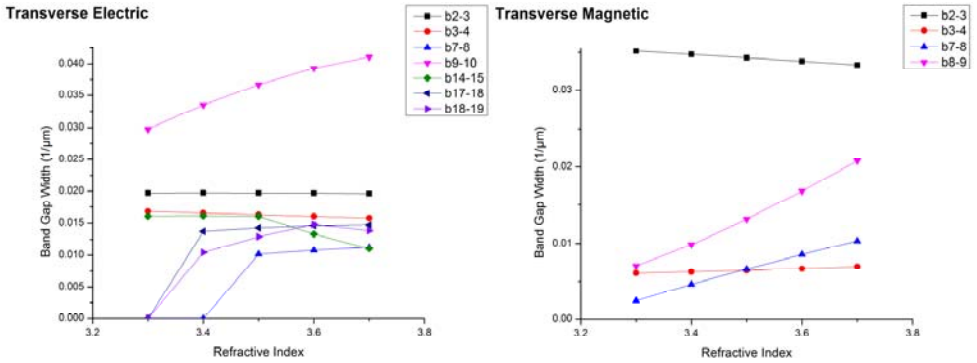

Fig. 4: Band gap distribution with respect to the higher refractive index

In the band gap distribution with respect to the refractive index (figure 4), we can observe the fact that 2 band gaps appear for TE, around the n_2=3.4 value, as for n_2=3.5, these two band gaps slightly increase and a third one emerges. A good transmission spectrum is suggested by both the width of a band gap and the number of gaps. The data shows that the higher the refractive index n_2 is, the crystal evolves towards developing complete band gaps, while the lower n_2 is, it allows light propagation for wider frequency intervals.

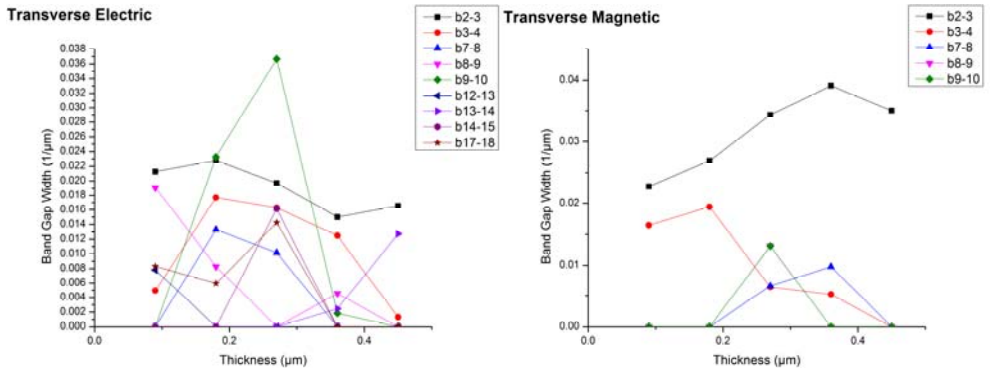

Fig. 5: Band gap distribution with respect to thickness of the material with n_2 refractive index

Analyzing the band gap distribution with respect to thickness (figure 5), we can observe that the sum of the gap widths is the highest in the middle point, which corresponds to a thickness of 0.27 μm for the material with the higher refractive index (n_2=3.5), and 0.33 μm for the material with the lower refractive index (n_1=1.4481). As we increased the thickness of the layer having a refractive index n_2, the crystal presents narrower band gaps, and higher transmission for both propagation modes.

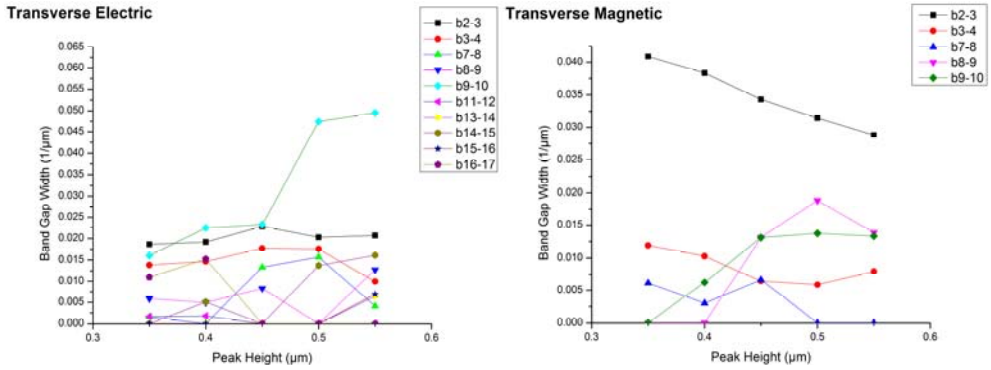

Fig. 6: Band gap distribution with respect to second peak's height

In the case of the band gap distribution with respect to second peak's height, at first sight, it would seem from figure 6 that the best results are shown by the highest peak height, due to a larger number of band gaps for TE and a lower band width for b2-3 and b7-8 for TM. However, the only two significant band width increases for TE is presented by b9-10 and b14-15. Three other significant band gaps (b2-3, b3-4, b7-8) present a lower width for a height of 0.55 μm than for a height of 0.45 μm. It can be observed that two other band gaps appear at a

height of 0.55 μm, although they do not affect the transmission spectrum significantly due to their small width.

After several simulations the results indicated that the optimal geometry has the following parameters: primitive cell dimensions: 1.2 μm length and 0.6 μm height, refractive indices: n_1=1.4481 and n_2=3.5, thickness: 0.2475 μm and 0.3525 μm respectively, peak heights: 0.9 μm and 0.45 μm respectively. The structure with the optimal geometry can be seen in figure 3 a), as previously stated.

The photonic band structure for the optimal geometry can be observed in figure 7, and the transmission spectra can be observed in figure 8, for both TE and TM. Both of these graphs have the same scale, in order to observe more clearly the difference between TE and TM. As mentioned above, we considered the wavelength interval of 0.66 – 2 μm, which means 0.5 – 1.5 1/μm on the vertical axis in figure 7.

As it can be observed, the crystal reveals a higher number of band gaps for TE and a significantly larger total band gap width in comparison to the TM mode. However, that is not the determining fact for the transmission spectra. As it can be observed, the band gap distribution for TE is rather uniform over the whole interval of interest, while for TM the band gaps group together in a certain interval indicating that the TM transmission will only be affected around that interval.

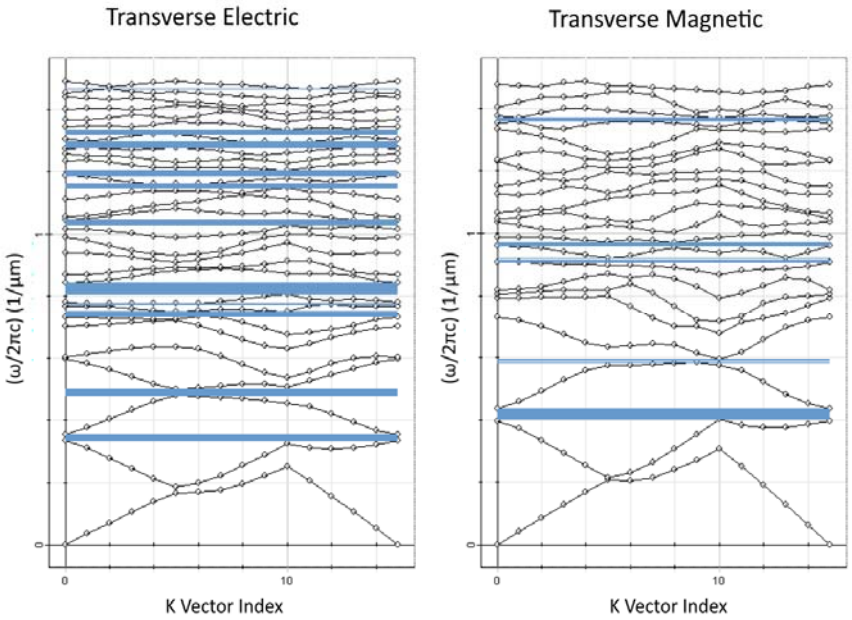

Fig. 7: Photonic Band Structures for the optimal geometry of the photonic crystal

Results from the band gap distributions were verified by calculating the transmission spectrum in each case. In this article we present only the transmission spectrum for the structure with optimal geometry in figure 8. It can be observed that the crystal acts as a linear polarizer over a large wavelength interval which spans from 0.66 μm to 1.9 μm. The transmission for the TE mode is very low, presenting variations below 3% of the source power over a wavelength interval from 0.66 μm to 1.65 μm, slightly increasing to 5% at 1.7 μm. Transmission for TE rapidly increases starting with 1.8 μm and presents no other variations until it reaches 1.95 μm.

The transmission spectrum for the TM mode presents strong, rising variations over an interval between 0.66 μm and 1.525 μm. In the interval between 1.525 μm and 1.8 μm there is a clear and definite difference between the transmissions for both propagation modes, where TM transmission varies slightly around 70% of the source power, reaching a maximum of 80% at 1.8 μm. Beyond this wavelength, we can observe a rapid switch in polarization, where TE rises to 48% and TM dropping to 2.5%, resulting in a TE polarized light for wavelengths in the interval 1.95 – 2 μm.

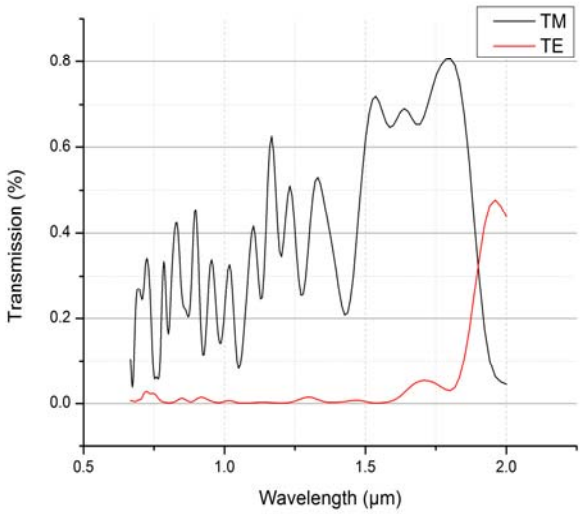

Fig. 8: Transmission spectra of TM and TE modes for the optimal geometry of the photonic crystal

4. Conclusions

We presented the evolution of photonic band gaps and transmissions for both TE and TM modes, with respect to several parameters that define a photonic crystal, which are the refractive index contrast, peak heights and film thickness. Our intention was to find a structure that would have the properties of a broadband linear polarizer. The crystal yielded best results for the following

parameters: n_1=1.4481, n_2=3.5, thicknesses: 0.3525 μm for the material with n_1, and 0.2475 μm for the material with n_2, peak heights: 0.9 μm and 0.45 μm. We have successfully designed a broadband linear polarizer using photonic crystals compatible with the autocloning technique [4] which acts in the wavelength interval of 0.66 – 1.9 μm. Using an appropriate substrate configuration we can produce a matrix of such photonic crystal linear polarizers for different directions, which will result in a polarization filter that can be used in a polarization imaging sensor.

R E F E R E N C E S

[1] *Viktor Gruev et al*, „Nano-wire Dual Layer Polarization Filter", IEEE International Symposium on Circuits and Systems, Taipei - Taiwan pp. 561-564, 2009;

[2] *Viktor Gruev et al*, „CCD polarization imaging sensor with aluminum nanowire optical filters", Optical Express, **vol. 18**, no. 18, pp. 19087-19094, 2010.

[3] *Alexander C. Edrington et al*, "Polymer-based Photonic Crystals", Advanced Materials, **vol. 13**, no. 6, pp. 421-425, 2001;

[6] *Daniel R. Solli et al*, „Photonic crystal polarizers and polarizing beam splitters", Journal of Applied Physics, **vol. 93**, no. 12, pp. 9429-9431, 2003;

[4] *H. L. Chen et al*, „Fabrication of autocloned photonic crystals by using high-density-plasma chemical vapor deposition", Journal of Vacuum Science and Technology, **vol. 22**, no. 6, pp. 3359-3363, 2004;

[5] *L. O'Faolain et al*, "Low-loss propagation in photonic crystal waveguides", Electronics Letters, **vol. 42**, no. 25, pp. 1454-1455, 2006;

[6] *T. Sato et al*, „Photonic crystals for the visible range fabricated by autocloning technique and their application", Optical and Quantum Electronics, **vol. 34**, no. 1-3, pp. 63-70, 2002;

[7] *M. Notomi et al*, "Waveguides, resonators and their coupled elements in photonic crystal slabs", Optics Express, **vol. 12**, no. 8, pp 1551-1561, 2004;

[8] *Bryce E. Bayer*, „Color Imaging Array", United States Patent, Appl. No. 555 477, 1976;

[9] *Viktor Gruev et al*, „Dual-tier thin polymer polarization imaging sensor", Optics Express, **vol. 18**, no. 18, pp. 19292-19303, 2010;